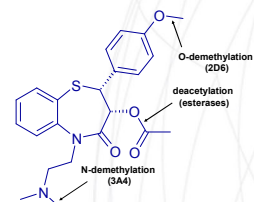


Physiologically-based pharmacokinetic (PBPK) modeling of diltiazem-midazolam drug-drug interaction (DDI)

Viera Lukacova, Michael Bolger, Walter Woltosz
Simulations Plus, Inc. Lancaster, California, USA,

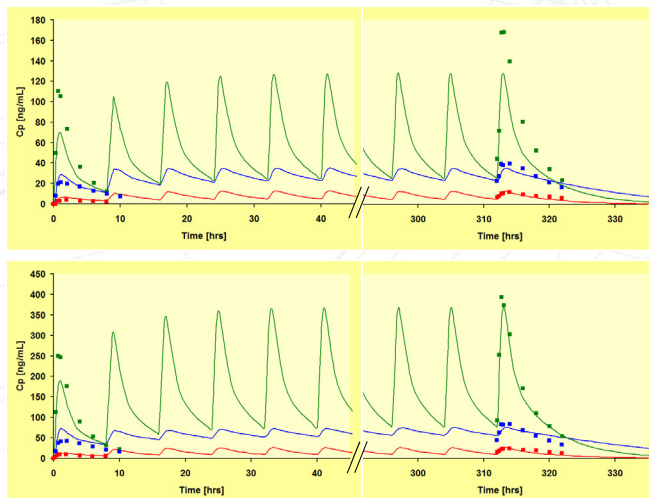
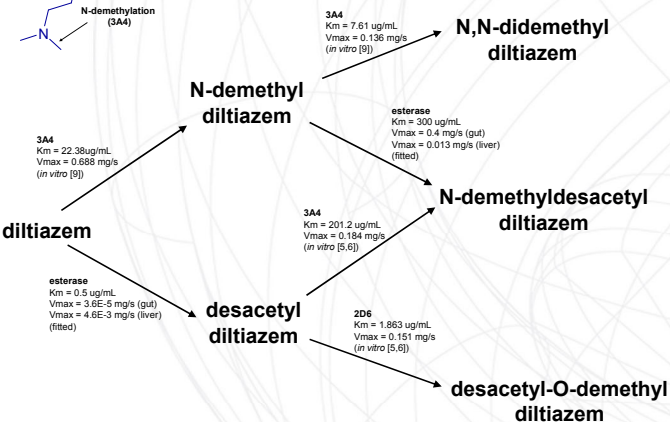
Abstract:

The purpose of this modeling effort was to explore the effects of various processes and physiological parameters on the DDI involving competitive and time-dependent inhibition (TDI). Absorption and pharmacokinetics of both drugs were simulated using GastroPlus™ 7.0 (Simulations Plus, Inc., Lancaster, CA). The program's Advanced Compartmental Absorption and Transit (ACAT™) model described the intestinal absorption, coupled with its PBPKPlus™ module for pharmacokinetic distribution and clearance. Human physiologies were generated by the program's internal Population Estimates for Age-Related (PEAR) Physiology™ module. Tissue/plasma partition coefficients were calculated using a modified Rodgers algorithm based on tissue composition and *in vitro* and *in silico* physicochemical properties (ADMET Predictor™, Simulations Plus, Lancaster, CA). Metabolic clearances of both drugs in gut and liver were based on built-in *in vitro* values for the expression levels of 3A4 in each gut compartment and the average expression of 3A4 in liver. Literature *in vitro* values for enzyme kinetic constants for 3A4 metabolism of midazolam, diltiazem and diltiazem metabolite were used as reported. Renal secretion of diltiazem and its metabolites was estimated as $f_{up} \times GFR$ and their residual clearances due to other metabolic processes were fitted to *in vivo* data. The PBPK models correctly described plasma concentration-time (Cp-time) profiles of midazolam, diltiazem and N-demethyldiltiazem for a variety of doses after *i.v.* and *p.o.* administration. Literature *in vitro* values for diltiazem inhibition constants were used as reported. Dynamic simulation within the DDI Module in GastroPlus was used to predict DDIs between the two drugs.

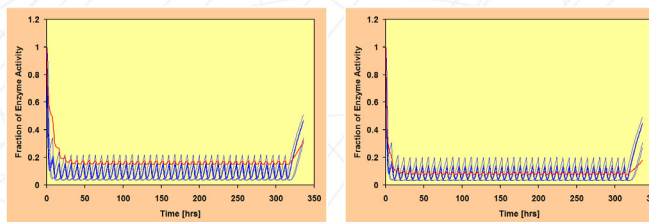


	K _i - rev [μM]	K _i - irrev [μM]	K _{inact} [min ⁻¹]
diltiazem	2.43	1.36	0.015
N-demethyl diltiazem	36.1	1.08	0.047

K_i - rev: reversible (competitive) K_i; K_i - irrev: irreversible K_i [8]



Predicted (solid lines) and observed (squares) plasma concentration-time profiles of diltiazem (green) and its two primary metabolites, N-demethyl diltiazem (blue) and desacetyl diltiazem (red), after *p.o.* administration of 60 mg (top) and 120 mg (bottom) doses of immediate release diltiazem every 8hrs.



Simulated changes in enzyme activity of 3A4 due to inactivation by diltiazem and N-demethyl diltiazem in gut (blue; each line represents one gut compartment) and liver (red) after *p.o.* administration of 60 mg (left) and 120 mg (right) doses of immediate release diltiazem every 8hrs.

References:

- Rodgers T.; J Pharm Sci 2007, 96: 3151-3152
- Rodgers T.; J Pharm Sci 2007, 96: 3153-3154
- Hoglund P.; Ther Drug Monitor 1989, 11: 543-550
- Hoglund P.; Ther Drug Monitor 1989, 11: 551-557
- Molden E.; Clin Pharmacol Ther 2002, 72: 333-342
- Molden E.; Drug Metab Dispos 2002, 30: 1-3
- Backman J.T.; Br J Clin Pharmac 1994, 37: 221-225
- Rowland-Yeo K.; Eur J Pharm Sci 2010, 39: 298-309
- Zhao P.; Drug Metab Dispos 2007, 35: 704-712

$$v = \frac{EnzAct_i \times V_{max} \times [S]_u}{K_m \left(1 + \frac{[I]_{u,D}}{K_{i,D}^{rev}} + \frac{[I]_{u,M}}{K_{i,M}^{rev}} \right) + [S]_u}$$

$$\frac{dEnzAct}{dt} = \left(\frac{k_{met,D} \times [I]_{u,D}}{K_{i,D}^{rev} \left(1 + \frac{[I]_{u,D}}{K_{i,D}^{rev}} \right) + [I]_{u,D}} + \frac{k_{met,M} \times [I]_{u,M}}{K_{i,M}^{rev} \left(1 + \frac{[I]_{u,D}}{K_{i,D}^{rev}} \right) + [I]_{u,M}} \right) \times EnzAct + k_{deg} (EnzAct_0 - EnzAct)$$

The model includes competitive (reversible) inhibition of the substrate's metabolic rate (v) by diltiazem (D) and N-demethyl diltiazem (M), as well as irreversible inhibition due to enzyme deactivation by both compounds. The effects of CYP 3A4 inactivation on the metabolism of diltiazem, N-demethyl diltiazem and desacetyl diltiazem, and their competition for binding sites of CYP 3A4, are also included in the model.

DDI Prediction Results:

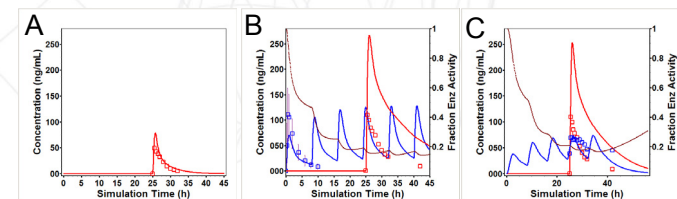
The pharmacokinetic model of diltiazem and its metabolites, as fitted against data from Hoglund [3,4], predicts an 80 and 90% decrease of 3A4 activity in liver after the *p.o.* administration of immediate release diltiazem doses of 60 mg and 120 mg, respectively.

Both doses resulted in gut 3A4 activity in the range of 0-20 % in different gut compartments.

The model predicted ~12 fold increase in midazolam AUC when midazolam was administered 1 hr after the 4th dose of diltiazem 60 mg dosing. This was significantly higher than the reported 4 fold increase in midazolam AUC [7].

A comparison of the *in vivo* diltiazem profiles as reported by Hoglund [3,4] and Backman [7] show significant differences after 60 mg *p.o.* administration every 8 hr, which might result in different effects on midazolam pharmacokinetics.

To determine if the diltiazem formulations used in the two studies might explain the differences in observed Cp-time profiles, an *in vivo* dissolution profile was fitted to the observed Cp-time profile from the Backman study [7]. It was determined that any differences in the release profiles between the two formulations were not able to completely explain the differences in diltiazem exposure. Additional effects due to physiological differences (e.g. different expression levels of involved enzymes) between the two populations are likely contributing to the difference. Unfortunately, the information in the Backman study [7] was not sufficient to account for these differences, as no metabolite profiles were reported.



Predicted (lines) and observed (points) Cp-time profiles of midazolam (red) after *p.o.* administration of 15 mg of midazolam with placebo (A) and diltiazem using the diltiazem pharmacokinetic model fitted to data reported by Hoglund (B) and Backman (C). Corresponding diltiazem concentration and CYP 3A4 activity profiles are shown in blue and brown, respectively.

Metabolic and inhibition parameters for diltiazem and its metabolites used in the model. All enzymes were included in both gut and liver. Additional nonspecific clearance due to other metabolism and/or renal clearance was added (fitted) for diltiazem, N-demethyl diltiazem and desacetyl diltiazem. When *in vitro* values were available, the same Vmax was applied to both gut and liver (scaled by different expression levels). Otherwise, separate Vmax values were fitted for gut and liver.

